

HARD X-RAY EMISSION FROM ACCRETION SHOCKS AROUND GALAXY CLUSTERS

DORON KUSHNIR¹ AND ELI WAXMAN¹

Draft version February 6, 2020

ABSTRACT

We show that the hard X-ray (HXR) emission observed from several galaxy clusters is naturally explained by a simple model, in which the nonthermal emission is produced by inverse Compton scattering of cosmic microwave background photons by electrons accelerated in cluster accretion shocks: The dependence of HXR surface brightness on cluster temperature is consistent with that predicted by the model, and the observed HXR luminosity is consistent with the fraction of shock thermal energy deposited in relativistic electrons being $\lesssim 0.1$. Alternative models, where the HXR emission is predicted to be correlated with the cluster thermal emission, are disfavored by the data. The implications of our predictions to future HXR observations (e.g. by NuStar, Simbol-X) and to (space/ground based) γ -ray observations (e.g. by Fermi, HESS, MAGIC, VERITAS) are discussed.

Subject headings: acceleration of particles - galaxies: clusters: general - radiation mechanisms: non-thermal - X-rays: general

1. INTRODUCTION

Nonthermal emission is observed from several clusters of galaxies, mainly in the radio band (e.g., Feretti & Giovannini 2008). In some cases, nonthermal hard (> 20 keV) X-ray (HXR) emission is also observed (for review, see Rephaeli et al. 2008). The radio emission is interpreted as synchrotron radiation, thereby suggesting that relativistic electrons and magnetic fields are present in the intracluster medium (ICM). The HXR emission is usually interpreted as due to inverse Compton (IC) scattering of cosmic microwave background (CMB) photons by nonthermal relativistic electrons (e.g., Rephaeli 1979; Sarazin 1999). In some cases, the HXR emission is also consistent with a two-temperature ICM (see Rephaeli et al. 2008, and references therein).

A clear identification of nonthermal HXR emission requires a precise measurement of the thermal emission, which dominates up to $\sim 30 - 40$ keV. We adopt in what follows the nonthermal HXR emission measurements reported in the literature, assuming that the subtraction of the thermal component has been performed correctly, and that the energy distribution of the nonthermal photons is well described by a power-law. We consider all reported measurements of HXR emission, excluding those where confusion with AGNs or radio galaxies (located within the field of view of the cluster observation) is possible (see § 2 for details). At present, data are available for 15 clusters satisfying this criterion.

Imaging information in the HXR band is at best limited. Thus, no clear identification of the nonthermal emitting source is available, and the measured flux must be considered as the flux generated by all sources within the instrument's field of view (FOV). One exception is the IBIS/ISGRI coded mask instrument aboard INTEGRAL, which was used to study the angular structure of the HXR emission of Coma (Eckert et al. 2007a; Lutovinov et al. 2008). At the "soft" 17–28.5 keV band, Coma is clearly an extended source. At the "hard"

44–107 keV band, the raw image does not show any significant substructure or correlation with the cluster's thermal emission (on 1° scale). The extended nature of the HXR emission implies that the radiating particles are not secondary particles produced in the interaction of cosmic-rays (CRs) with the ICM, since the generation of such secondary particles should be strongly concentrated towards the cluster's center.

Several models for the HXR emission from clusters have been presented in the literature. These models differ in the assumptions regarding the nonthermal emission mechanism as well as regarding the origin of the emitting electrons. In some models, the nonthermal emission mechanism is IC scattering of CMB photons by relativistic electrons (e.g., Rephaeli 1979; Sarazin 1999; Colafrancesco & Marchegiani 2009), while in others the mechanisms are nonthermal bremsstrahlung (e.g., Sarazin 1999; Sarazin & Kempner 2000) or synchrotron emission from ultra-relativistic electrons (Timokhin et al. 2004; Inoue et al. 2005; Eckert et al. 2007b). Various sources have been suggested for the emitting electrons: a population of point sources (e.g. AGN as in Katz 1976; Fabian et al. 1976; Fujita et al. 2007), merger shocks (e.g., Fujita et al. 2003; Brunetti et al. 2004), dark matter bow shocks (e.g., Bykov et al. 2000), ram-pressure stripping of infalling galaxies (e.g., de Plaa et al. 2006) and accretion shocks (e.g., Loeb & Waxman 2000; Fujita et al. 2003; Berrington & Dermer 2003; Gabici & Blasi 2003; Brunetti et al. 2004; Inoue et al. 2005; Kushnir & Waxman 2009).

We note here that the nonthermal radio emission is unlikely to be produced by the same population of electrons producing the nonthermal HXR emission (as suggested in some models, e.g. Rephaeli 1977, 1979). Requiring the same electrons to produce both the HXR and radio emission requires ICM magnetic fields which are very weak compared to those inferred from Faraday rotation measurements (Kim et al. 1991) and compared to those estimated based on the correlation between the radio flux and the cluster thermal X-ray flux (Kushnir et al. 2009).

In this paper we show that all available cluster HXR

¹ Physics Faculty, Weizmann Institute of Science, Rehovot, Israel

observations are naturally explained by a simple analytic model (Loeb & Waxman 2000; Kushnir & Waxman 2009), in which the HXR emission is due to IC scattering of CMB photons by relativistic electrons accelerated in accretion shocks surrounding the clusters. The cluster sample that we use is described in § 2. In § 3 we briefly describe the model, and compare its predictions with the observations (for a detailed description of the model, the reader is referred to Kushnir & Waxman 2009). In § 4 we show that alternative models, in which the HXR emission is predicted to be correlated with the cluster thermal emission, are disfavored by the data. In particular, in models where the radiating electrons are secondaries produced in inelastic nuclear p-p collisions, the energy in CR protons is required to exceed the thermal energy of the gas, which is both unlikely and inconsistent with the observed correlation between the radio flux and the thermal X-ray flux (Kushnir et al. 2009). Our results are summarized and their implications are discussed in § 5.

Throughout, a Λ CDM cosmological model is assumed with $H_0 = 70h_{70} \text{ km s}^{-1} \text{ Mpc}^{-1}$, $\Omega_m = 0.23$, $\Omega_b = 0.039$ and $\Omega_\Lambda = 1 - \Omega_m$. Due to the small redshift range of the observed clusters, we neglect redshift dependencies where justified.

2. OBSERVATIONS

We use the compilation of Rephaeli et al. (2008) for the RXTE, BeppoSAX and INTEGRAL observations, the results of Ajello et al. (2009) for the Swift/BAT observations and the results of Wik et al. (2009) for the SUZAKO observations. We consider 6 clusters observed with RXTE (in the 20 – 80 keV band), 4 clusters observed with BeppoSAX (20 – 80 keV), 1 cluster observed with INTEGRAL (44–107 keV), 8 clusters observed with Swift/BAT (50 – 100 keV) and 1 cluster observed with SUZAKO (12–70 keV), where the Coma cluster has been observed with all five instruments and A2256 with two. Our sample includes therefore a total of 15 different clusters, for which HXR detection or upper limits are available. Most of the clusters show clear signs of a recent merger (this may bias the inferred model parameter values, see discussion in § 5).

Different instruments are sensitive over different X-ray energy ranges. When comparing the measurements of different instruments we therefore compare the flux per logarithmic energy interval of X-ray photons, i.e. the flux divided by $\Lambda \equiv \log(\nu_{\text{max}}/\nu_{\text{min}})$ where $h\nu_{\text{max,min}}$ are the upper and lower bounds respectively of the instrument’s energy band. For the relevant instruments, Λ is within the range 0.7 – 1.8. Our choice is motivated by the fact that a photon spectral index of 2, i.e. $dn_\gamma/d\varepsilon_\gamma \propto \varepsilon_\gamma^{-2}$, is expected in our model (see § 3) and is also consistent with observations (note, however, that there are large uncertainties in the observational determination of the spectral index, e.g. Rephaeli et al. 2008). For such a spectrum, the flux per logarithmic energy interval is independent of energy.

The different instruments differ also in their FOV. The FOV radii of RXTE, BeppoSAX and INTEGRAL are in the range of 30’ to 60’, and those of Swift/BAT and SUZAKO are smaller, $\sim 10'$. Since these FOV radii are comparable to the characteristic sizes of massive clusters (lying at distances of few 100 Mpc), the HXR flux measurements obtained by instruments with differing FOVs

provide some information on the intra-cluster spatial distribution of the HXR emission. Models in which the HXR emission follows the thermal emission predict that the HXR flux should not significantly vary as the FOV grows to include cluster regions beyond the cluster core, since the thermal emission is strongly dominated by the core. On the other hand, models in which the HXR surface brightness is roughly uniform across the cluster, or rising away from the cluster center (as predicted by the model described in § 3), predict that the HXR flux should increase significantly as the FOV grows beyond the angular size of the core. As we show in § 4, the data support the latter qualitative behavior, therefore suggesting that the HXR emission is extended and not dominated by the cores of the clusters.

3. A SIMPLE MODEL FOR THE HXR EMISSION

Let us first briefly describe the main assumptions, and the main relevant results, of the model discussed by Kushnir & Waxman (2009) for the nonthermal emission produced by cluster accretion shocks. In this model, it is assumed that matter is accreted onto a cluster of mass M at a rate $\dot{M} = f_{\text{inst}} M_{200}/t_H$, where t_H is the (instantaneous) Hubble time, M_{200} is the mass contained within a radius r_{200} , within which the mean density is 200 times the critical density ρ_{crit} , and f_{inst} is a dimensionless parameter of order unity, reflecting the temporal fluctuations of $\dot{M}/(M_{200}/t_H)$. As discussed in (Kushnir & Waxman 2009), 3D numerical simulations indicate that the average value of f_{inst} is ≈ 0.5 . The accreted gas is assumed to be shocked to the cluster’s virial temperature T (see discussion in § 5). Since the accretion shock is strong and collisionless, it is assumed that it produces a nonthermal population of relativistic electrons, with an energy spectrum (e.g., Blandford & Eichler 1987)

$$dn/d\varepsilon \propto \varepsilon^{-2}. \quad (1)$$

The fraction of the post shock thermal energy density carried by relativistic electrons is denoted by η_e .

The accelerated electrons lose energy by IC scattering of CMB photons (which dominates over synchrotron emission at the accretion shock). At sufficiently high energies, where the electron cooling time is short compared to the time scale for cluster evolution, the resulting IC luminosity per logarithmic photon energy interval is simply given by

$$\nu L_\nu^{\text{IC,shock}} = \frac{1}{2} \frac{3}{2} \frac{\eta_e f_b T}{\Lambda_e} f_{\text{inst}} \frac{M_{200}}{\mu m_p t_H}, \quad (2)$$

where $f_b = \Omega_b/\Omega_m$, μm_p is the average mass of shocked plasma particles, and $\Lambda_e \sim 20$ is the number of logarithmic energy intervals in the energy spectrum of the relativistic electrons. The frequency at which an electron emits most of its IC power is given by $\nu = \nu_0 \gamma^2$, where $\nu_0 = 3T_{\text{CMB}}/h$, T_{CMB} is the CMB temperature and γ is the Lorentz factor of the electron. The Lorentz factor of electrons emitting HXR photons of energy ε_{HXR} is

$$\gamma_{\text{HXR}} \approx 5.3 \times 10^3 \left(\frac{\varepsilon_{\text{HXR}}}{20 \text{ keV}} \right)^{1/2}, \quad (3)$$

and their cooling time is

$$t_{\text{cool}} \approx 0.44 \left(\frac{\varepsilon_{\text{HXR}}}{20 \text{ keV}} \right)^{-1/2} \text{ Gyr}. \quad (4)$$

Thus, the cooling time of electrons emitting at the HXR band is short compared to the clusters' evolution time, and the IC luminosity at the HXR band is well approximated by eq. (2).

In order to determine the cluster's HXR luminosity (and surface brightness) as function of its temperature T , a relation between T and M_{200} (and r_{200}) should be used. The density profile of the X-ray emitting ICM is generally well described by a " β -model" (Cavaliere & Fusco-Femiano 1976; Gorenstein et al. 1978; Jones & Forman 1984),

$$\rho_{\text{gas}}(r) \propto \left(1 + \frac{r^2}{r_c^2}\right)^{-(3/2)\beta}, \quad (5)$$

where r_c is the X-ray core radius. Assuming the ICM plasma to be isothermal and in hydrostatic equilibrium gives

$$\begin{aligned} r_{200} &\sim \left(\frac{800\pi}{3}\rho_{\text{crit}}\right)^{-1/2} \left(\frac{3\beta T}{\mu m_p G}\right)^{1/2} \\ &\sim 3.1\beta^{1/2}T_1^{1/2}h_{70}^{-1} \text{ Mpc}, \\ M_{200} &\sim \left(\frac{800\pi}{3}\rho_{\text{crit}}\right)^{-1/2} \left(\frac{3\beta T}{\mu m_p G}\right)^{3/2} \\ &\sim 3.5 \cdot 10^{15}\beta^{3/2}T_1^{3/2}h_{70}^{-1}M_{\odot}. \end{aligned} \quad (6)$$

Here, $T_1 = T/10$ keV and $\mu \sim 0.59$ is the mean molecular weight for fully ionized gas with hydrogen mass fraction of $\chi = 0.75$. We assume that the accretion shock is located at $r \sim r_{200}$, since spherical collapse models predict a cluster virial density $\langle \rho_{\text{vir}} \rangle \simeq 178\rho_{\text{crit}}$ for $\Omega_m = 1$, $\Omega_{\Lambda} = 0$ (with weak dependance on the background cosmology for the relevant range $0.3 \lesssim \Omega_m < 1$).

In addition to the assumption that the ICM is isothermal and in hydrostatic equilibrium, we have assumed in deriving eq. (6) that the density profile is given by eq. (5) out to r_{200} . This implies $\rho \propto r^{-2}$ at large radii, in contrast with the $\rho \propto r^{-3}$ dependence expected at large r (e.g. Navarro et al. 1997). However, a detailed discussion of the accuracy of cluster mass determination under these approximations, given in Reiprich & Bohringer (2002), shows that eq. (6) may overestimate M_{200} by no more than 20%.

Since most of the clusters observed in HXR have recently undergone a merger, a note is in place concerning the validity of our approximate description of cluster properties (eqs. 2, 5, 6). X-ray cluster maps (e.g., Finoguenov et al. 2005) show that both relaxed and unrelaxed clusters are not simple hydrostatic equilibrium systems. Particularly, the structure of recently merged clusters often deviates from a hydrostatic equilibrium. However, since the deviations of the gas profiles from the mean hydrostatic equilibrium profiles are at the few tens of percent level, we expect our description to be approximately valid. Detailed analysis of numerical simulations of cluster mergers (e.g. Ricker & Sarazin 2001; Poole et al. 2006, 2007) can be used to determine the effects of deviations from our simple approximate description.

Using eq. (6), the accretions shock luminosity, eq. (2),

gives

$$\begin{aligned} \nu L_{\nu}^{\text{IC,shock}} &= 1.7 \cdot 10^{44} (f_{\text{inst}}\eta_e)_{-1} \beta^{3/2} \\ &\times \left(\frac{f_b}{0.17}\right) T_1^{5/2} \text{ erg s}^{-1}, \end{aligned} \quad (7)$$

where $(f_{\text{inst}}\eta_e)_{-1} = f_{\text{inst}}\eta_e/10^{-1}$. Assuming that the HXR emission originates in a thin shell lying at the shock radius, the HXR flux of a cluster at a distance $d \simeq cz/H_0$, within the energy band $[\varepsilon_1, \varepsilon_2]$ and within a disk of angular radius θ centered at the cluster center, is given by

$$\begin{aligned} F_{[\varepsilon_1, \varepsilon_2]}(\theta) &= 7.5 \cdot 10^{-8} (\langle f_{\text{inst}} \rangle_{\theta} \eta_e)_{-1} \beta^{1/2} \\ &\times \left(\frac{f_b}{0.17}\right) T_1^{3/2} \Lambda g_{\text{acc.}}(\theta) h_{70}^2 \frac{\text{erg}}{\text{cm}^2 \text{s}}, \end{aligned} \quad (8)$$

where

$$g_{\text{acc.}}(\theta) = 2\theta_{200}^2 \left[1 - \sqrt{1 - \left(\frac{\theta}{\theta_{200}}\right)^2}\right]. \quad (9)$$

Here $\theta_{200} = r_{200}/d$ and we have used $\langle f_{\text{inst}} \rangle_{\theta}$, defined as the average value of f_{inst} over the disk considered, to explicitly reflect the possible spatial dependence of the accretion mass flux.

Eq (9) gives an approximate description of the dependence of F on θ , for the case where the emission takes place within a shell of radius $r = r_{200}$ and thickness $w \ll r_{200}$. The thickness of the emitting region is approximately given by the product of the cooling time of the emitting electrons and the velocity of the downstream fluid relative to the shock velocity, u_d . Using $u_d = \sqrt{T/3\mu m_p} \simeq 7.4 \cdot 10^2 T_1^{1/2} \text{ km s}^{-1}$, we have

$$\begin{aligned} w &\simeq u_d t_{\text{cool}} \\ &\simeq 3.3 \cdot 10^2 T_1^{1/2} \left(\frac{\varepsilon_{\text{HXR}}}{20 \text{ keV}}\right)^{-1/2} \text{ kpc}. \end{aligned} \quad (10)$$

This confirms that $w \ll r_{200}$. For $w = 0.1r_{200}$, eq. (9) is accurate to better than $\sim 25\%$ for any θ .

Eq. (8) predicts that $F/\Lambda g_{\text{acc.}}$ should scale as $(T_1\beta^{1/3})^{3/2}$, with a normalization that depends on $\langle f_{\text{inst}} \rangle_{\theta} \eta_e$. The model predictions are compared with observations in figure 1, where we show the measurements and upper-limits of $F/\Lambda g_{\text{acc.}}$ for the entire sample, and in figure 2, where we show only clusters with HXR detections (The vertical error bars reflect only the uncertainty in measured fluxes, F ; we ignored the errors in the determination of $g_{\text{acc.}}$, which are significantly smaller). A linear fit for $\ln(F/\Lambda g_{\text{acc.}})$ as function of $\ln(T\beta^{1/3})$ gives a slope of 1.4 ± 0.5 , consistent with the predicted slope of $3/2$. For a slope of $3/2$, the best linear fit is obtained for $f_{\text{inst}}\eta_e \sim 0.2$. The small deviations (up to a factor of 2) from a constant $f_{\text{inst}}\eta_e$ line could result from cluster-to-cluster variations of f_{inst} , or from variations of the accretion flow across individual clusters (note that different instruments have different FOV).

4. OTHER MODELS

In the preceding section we presented a simple model for the HXR emission from galaxy clusters, and have shown that it naturally explains the available HXR cluster data. In this section we consider alternative models, in which the HXR emission is predicted to be correlated

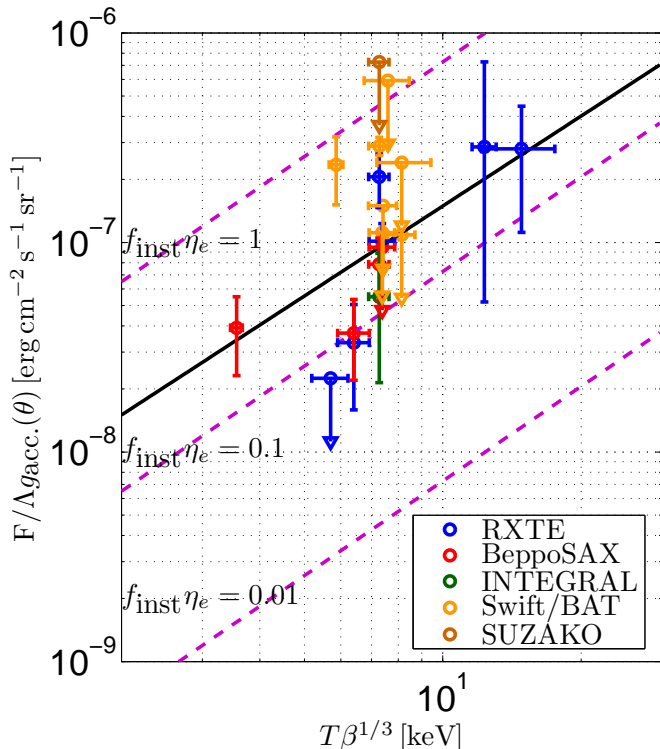


FIG. 1.— $F/\Lambda g_{\text{acc.}}$ as function of $T\beta^{1/3}$ (see eq. 8). A linear fit for $\ln(F/\Lambda g_{\text{acc.}})$ as function of $\ln(T\beta^{1/3})$ gives a slope of 1.4 ± 0.5 , consistent with the predicted slope of $3/2$. For a slope of $3/2$, the best linear fit is obtained for $f_{\text{inst}}\eta_e \sim 0.2$. In deriving the fits, we used average values (over all instruments) for the Coma and A2256 fluxes, and disregarded the Swift/BAT measurement, for which the existence of a nonthermal component is uncertain (Ajello et al. 2009). The best fit is shown by the solid black line. Constant $f_{\text{inst}}\eta_e$ lines are shown as dashed magenta lines.

with the cluster thermal emission. In such models, the HXR emission should be strongly dominated by emission from the cluster’s core, which dominates the thermal X-ray emission. This is in contrast with the predictions of the model described in § 3, in which the HXR emission is produced at the cluster accretion shock. In the latter model, the HXR surface brightness is expected to be nearly uniform across the cluster, and enhanced along the (apparent) accretion shock ring (see eq. 9).

One indication that the HXR emission is extended, and not dominated by the cluster core, is provided by the INTEGRAL imaging observations of the Coma cluster, where the raw hard-band image does not show any significant substructure (see § 1). The lack of a correlation between the HXR emission and the thermal X-ray emission disfavors models in which the thermal and non-thermal X-ray emission are strongly correlated. We show below that a similar conclusion is reached by analyzing the data available for the sample of 15 clusters discussed in this paper.

A widely discussed model for the HXR emission, which predicts the HXR emission to be proportional to the thermal emission, is a model in which the relativistic electrons are secondaries produced by inelastic p-p collisions between cluster CRs and thermal intra-cluster gas (e.g., Rephaeli 1979). We therefore consider this model in some detail below. As explained at the end of this

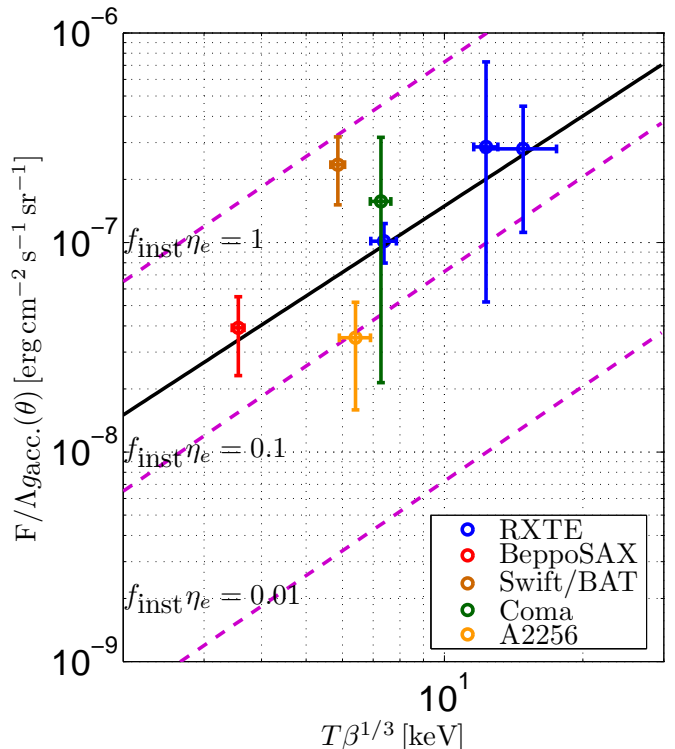


FIG. 2.— Same as figure 1, including only clusters with HXR detections, and average (over all instruments) values for the Coma and A2256 clusters.

section, our conclusion, that the data indicate that the spatial distributions of the HXR and of the thermal X-ray emission are different, is general and apply not only to the secondary electron model.

In the secondary electron model, the ICM is assumed to contain a population of proton CRs with a power law energy distribution $\varepsilon^2 dn_{\text{CR}}/d\varepsilon = \beta_{\text{core}} 3nT/2$, where n is the ICM number density and β_{core} is the ratio between the CR energy (per logarithmic particle energy interval) and the thermal energy. The HXR luminosity per logarithmic frequency interval is proportional in this model to the X-ray luminosity (see Kushnir & Waxman 2009, for details),

$$\frac{\nu L_{\nu}^{\text{sec}}}{L_X} \simeq 1.1 \cdot 10^{-5} \beta_{\text{core},-4} T_1^{1/2} \frac{B_{\text{CMB}}^2}{B_{\text{CMB}}^2 + B^2}, \quad (11)$$

where $\beta_{\text{core},-4} = \beta_{\text{core}}/10^{-4}$ and B is the intra-cluster magnetic field. $B_{\text{CMB}} \equiv (8\pi a T_{\text{CMB}}^4)^{1/2} \approx 3.2 \mu\text{G}$ is the magnetic field, for which the magnetic energy density equals the energy density of the CMB. Note, that in contrast with the magnetic field at the accretion shock, which is much smaller than B_{CMB} , the magnetic field at the cluster core is expected to be $\geq B_{\text{CMB}}$.

The flux within a disk of angular radius θ for a cluster at a distance $d \sim cz/H_0$ is given (for $\beta > 0.5$, see Sarazin & Bahcall 1977) by

$$F_{[\varepsilon_1, \varepsilon_2]}(\theta) = 5.4 \cdot 10^{-15} h_{70}^2 \times T_1^{1/2} L_{X,45.5} \Lambda g_{\text{therm.}}(\theta) \times \begin{cases} B_{-5}^{-2}, & B \gg B_{\text{CMB}} \\ 0.1, & B \ll B_{\text{CMB}} \end{cases} \beta_{\text{core},-4} \frac{\text{erg}}{\text{cm}^2 \text{s}}, \quad (12)$$

where

$$g_{\text{therm.}}(\theta) = \left(3\beta - \frac{3}{2}\right) \left(\frac{z}{z_{\text{Coma}}}\right)^{-2} \times \int_0^{\min(\theta d/r_c, r_{200}/r_c)} \frac{\bar{r} d\bar{r}}{(1 + \bar{r}^2)^{3\beta - 1/2}}. \quad (13)$$

Here $L_{X,45.5} = h_{70}^2 L_X / 3 \cdot 10^{45} \text{ erg s}^{-1}$, $\beta_{\text{core},-4} = \beta_{\text{core}} / 10^{-4}$, and $B_{-5} = B / 10 \mu\text{G}$. In order to obtain an analytic relation between the luminosity and the surface brightness, we have assumed in deriving equations (12) and (13) that the cluster emission extends to infinite radius. For β values close to 0.5, the derived relation deviates significantly from the one that would be obtained assuming that the emission is strongly suppressed beyond r_{200} . For clusters with β close to 0.5 we do not use, therefore, eq. (13), but rather the relation obtained assuming emission is truncated beyond r_{200} .

In the secondary model, $F/\Lambda g_{\text{therm.}}$ scales as $T_1^{1/2} L_{X,45.5}$, with normalization that depends on $B^{-2} \beta_{\text{core}}$ (or only on β_{core} if $B \ll B_{\text{CMB}}$). In figure 3 we show $F/\Lambda g_{\text{therm.}}$ as function of $T_1^{1/2} L_{X,45.5}$ (Vertical error bars reflect only the uncertainty in measured fluxes, F ; we ignored the errors in the determination of $g_{\text{therm.}}$, which are significantly smaller). Comparing the detected HXR emission with the constant $B^{-2} \beta_{\text{core}}$ (or β_{core}) lines of the figure, we find that $B_{-5}^{-2} \beta_{\text{core},-4} = 10^4$ (or $\beta_{\text{core},-4} = 10^3$ for $B \ll B_{\text{CMB}}$) is required in order to account for the observed fluxes. This implies that the total energy density of CR protons, $\log(\varepsilon_{\text{max}}/\varepsilon_{\text{min}}) \times \beta_{\text{core}} \approx 20\beta_{\text{core}}$, should exceed the thermal energy density of the gas in order for the emission from secondary electrons to account for the observed HXR emission. This strongly disfavors the secondary electron model. Moreover, the correlation between the radio and thermal X-ray emission of galaxy clusters was shown (Kushnir et al. 2009) to imply that the typical value of β_{core} is $\simeq 2 \times 10^{-4}$ and that $B \gg B_{\text{CMB}}$ for clusters which host radio halos.

Examining fig. 3, we find that the Swift/BAT detection and upper limits on $F/\Lambda g_{\text{therm.}}$ are well below the values of $F/\Lambda g_{\text{therm.}}$ inferred for clusters with similar T from the detections of other instruments. The systematically lower HXR fluxes derived from the Swift measurements are naturally explained by the model described in § 3, in which the HXR emission is extended and not dominated by the cluster core. In this case, the lower Swift fluxes are due to its smaller FOV. Figure 1 demonstrates that this is a valid explanation (the upper limits on $F/\Lambda g_{\text{acc.}}$ obtained by Swift are consistent with the values of $F/\Lambda g_{\text{acc.}}$ inferred from the detection of other instruments). The lower HXR fluxes implied by Swift's observations may also be explained by assuming that the clusters observed by Swift are intrinsically different (e.g. having significantly lower values of $f_{\text{inst}} \eta_e$) than those observed by other instruments. Since we have no reason to assume that the Swift clusters are systematically different than those observed by other instruments (all are prominently merging clusters), we conclude that the data disfavor all models, in which the spatial distribution of the HXR and of the thermal X-ray emission are strongly correlated.

5. DISCUSSION

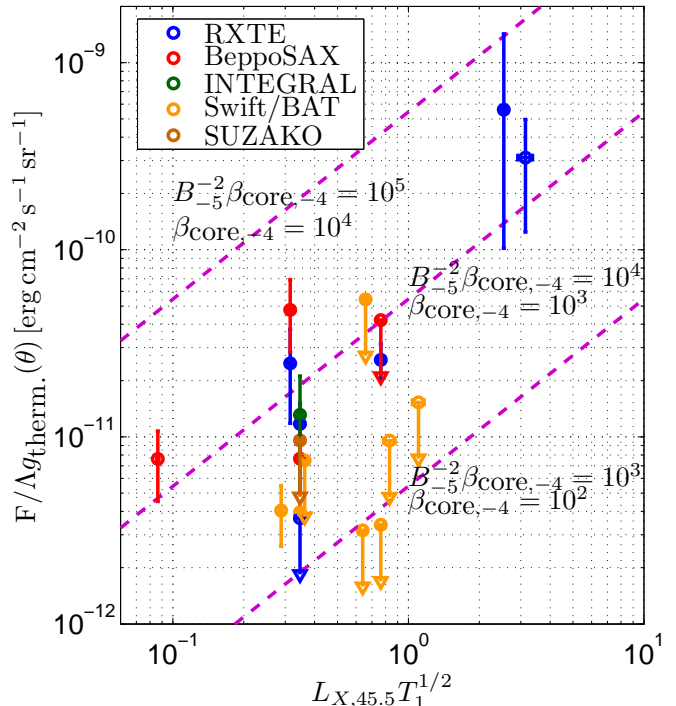


FIG. 3.— $F/\Lambda g_{\text{therm.}}$ as function of $T_1^{1/2} L_{X,45.5}$. Dashed magenta lines show constant values of $B^{-2} \beta_{\text{core}}$ (or β_{core} , see eq. 12).

We have presented in § 3 a simple model, that explains the HXR emission from galaxy clusters as IC scattering of CMB photons by relativistic electrons accelerated in the accretion shock surrounding the cluster: The correlation predicted in this model between the HXR surface brightness and the cluster temperature is consistent with the observations, and the observed HXR luminosity is consistent with the fraction η_e of shock thermal energy deposited in relativistic electrons being $\eta_e \sim 0.1$ (see fig. 2). The implied acceleration efficiency of electrons is similar to the acceleration efficiency of protons in the accretion shocks, which is inferred from the correlation between the radio flux and the thermal flux of galaxy clusters (Kushnir et al. 2009). The nonthermal luminosity and surface brightness produced by the accretion shock are given in this model by eqs. (7) and (8).

Several comments are in place here regarding the estimated value of η_e . HXR observations do not allow one to determine η_e directly. Rather, such observations constrain directly only the value of the product $\eta_e f_{\text{inst}}$, where f_{inst} is the mass accretion rate measured in units of M_{200}/t_H (see eq. (7)). We have found that the observed HXR fluxes are consistent with $\eta_e f_{\text{inst}} \sim 0.1$. However, since the sample of clusters for which HXR observations are available is not complete, the inferred value of $\eta_e f_{\text{inst}} \sim 0.1$ may be biased, i.e. may differ from its average value (over all clusters). In particular, since most of the clusters chosen for HXR observations are merging systems, in which enhancement of the accretion rate is expected (see e.g., Pfrommer et al. 2008), the inferred value of $\eta_e f_{\text{inst}}$ is probably biased in the current sample towards values higher than average. De-

termination of the average value of f_{inst} from numerical simulations and using a complete cluster sample, that may be produced by future HXR missions (e.g. NuStar, Simbol-X), would allow one to estimate the value η_e more accurately.

Another limitation of the estimate of η_e should be mentioned. We have assumed in our analysis that the ICM plasma is isothermal and in hydrostatic equilibrium. Deviations from this simple model near the virial radius may change our estimates for η_e . Although such deviations are only weakly constrained by observations, both observational (e.g. Vikhlinin et al. 2005) and theoretical (e.g. Roncarelli et al. 2006) analyses indicated that they are not large (for example, the accretion shock temperature is lower than the virial temperature by no more than a factor ~ 2). Modifications of the ICM properties near the virial radius may be easily incorporated into our model. Improved (observational) determination of the ICM profile near the virial radius will therefore allow one to improve the accuracy of the determination of η_e .

Our model predicts the HXR surface brightness to be nearly uniform across the cluster, and enhanced along the (apparent) accretion shock ring (see eq. 9). This is in contrast with models, in which the HXR emission is strongly correlated with the thermal X-ray emission, that is dominated by the cluster's core. We have shown in § 4 that the low values of HXR flux inferred from Swift's observations disfavor models, in which the HXR emission is dominated by the cores of the clusters: For an extended HXR emission, the low Swift fluxes are naturally explained as due to the smaller FOV of Swift, while for emission dominated by the cores of clusters the flux should not depend strongly on the FOV (see last paragraph of § 4 and compare figures 1 and 3). Moreover, it was shown in § 4 that a widely discussed model for HXR emission, in which the relativistic electrons producing the radiation are secondaries produced by inelastic p-p collisions between cluster CRs and thermal ICM (e.g., Rephaeli 1979), requires the total energy density of CRs to exceed the thermal energy density of the ICM. This strongly disfavors the secondary electron model.

Our model prediction, that the HXR emission is extended, may be tested by future HXR missions capable of producing high resolution HXR maps of clusters (NuStar

and Simbol-X, e.g., may reach a resolution of tens of arcsec). This prediction could also be tested by future γ -ray observations. Our model predicts that cluster accretion shocks produce a γ -ray flux of (see eq. (8))

$$F_{\nu > \nu_{\text{min}}}^{\text{IC,shock}}(\theta) = 4.7 \cdot 10^{-6} (\langle f_{\text{inst}} \rangle \theta \eta_e)_{-1} \beta^{1/2} \\ \times \left(\frac{f_b}{0.17} \right) T_1^{3/2} \left(\frac{\varepsilon_{\nu, \text{min}}}{10 \text{ GeV}} \right)^{-1} \\ \times g_{\text{acc.}}(\theta) h_{70}^2 \text{ ph cm}^{-2} \text{ s}^{-1}. \quad (14)$$

This flux, which is marginally detectable by EGRET (see detailed discussion for the Coma cluster in Kushnir & Waxman 2009), should be easily detectable by Fermi, which has a ~ 50 times higher sensitivity and which may resolve the cluster (the angular resolution of Fermi reaches 0.1° above 10 GeV, see <http://www-glast.stanford.edu/>).

Imaging Cerenkov telescopes may also detect the predicted nonthermal flux. However, it should be noted that flux predictions for energies > 1 TeV are uncertain. ~ 1 TeV photons are expected to be produced by the highest energy electrons accelerated in the accretion shocks (Loeb & Waxman 2000). Since, however, our estimate of the cutoff energy of the electrons is not robust (see Keshet et al. 2003, for details), the > 1 TeV flux may fall well below the prediction of eq. (14). Lowering the energy threshold of the imaging Cerenkov telescopes to ~ 0.1 TeV would be very helpful in this context, since the prediction of eq. (14) is more reliable at photon energies $\ll 1$ TeV. It is important to mention here that measurements of the nonthermal emission in different energy bands (e.g. HXR and γ -rays) would allow one to constrain the energy distribution of the accelerated electrons.

We finally note that our estimates for the IC flux cannot be used directly for the Soft X-ray band (< 1 keV), since the cooling time of the emitting electrons may exceed the dynamical time of the cluster (see eq. (4)).

This research was partially supported by AEC, Minerva and ISF grants.

REFERENCES

- Ajello, M. et al. 2009, ApJ, 690, 367, 0809.0006
 Berrington, R., & Dermer, C. 2003, ApJ, 594, 709
 Blandford, R., & Eichler, D. 1987, Phys. Rep., 154, 1
 Brunetti, G., Blasi, P., Cassano, R., & Gabici, S. 2004, MNRAS, 350, 1174, arXiv:astro-ph/0312482
 Bykov, A. M., Bloemen, H., & Uvarov, Y. A. 2000, A&A, 362, 886
 Cavaliere, A., & Fusco-Femiano, R. 1976, A&A, 49, 137
 Colafrancesco, S., & Marchegiani, P. 2009, ArXiv e-prints, 0904.3429
 de Plaa, J. et al. 2006, A&A, 452, 397, arXiv:astro-ph/0602582
 Eckert, D., Neronov, A., Courvoisier, T. J.-L., & Produit, N. 2007a, A&A, 470, 835, 0705.2722
 Eckert, D., Produit, N., Neronov, A., & Courvoisier, T. J. . 2007b, ArXiv e-prints, 0710.4417
 Fabian, A. C., Pringle, J. E., & Rees, M. J. 1976, Nature, 263, 301
 Ferretti, L., & Giovannini, G. 2008, in Lecture Notes in Physics, Berlin Springer Verlag, Vol. 740, A Pan-Chromatic View of Clusters of Galaxies and the Large-Scale Structure, ed. M. Plionis, O. López-Cruz, & D. Hughes, 143–+
 Finoguenov, A., Böhringer, H., & Zhang, Y.-Y. 2005, A&A, 442, 827, arXiv:astro-ph/0507452
 Fujita, Y., Kohri, K., Yamazaki, R., & Kino, M. 2007, ApJ, 663, L61, 0705.4284
 Fujita, Y., Takizawa, M., & Sarazin, C. L. 2003, ApJ, 584, 190, arXiv:astro-ph/0210320
 Gabici, S., & Blasi, P. 2003, ApJ, 583, 695
 Gorenstein, P., Fabricant, D., Topka, K., Harnden, Jr., F. R., & Tucker, W. H. 1978, ApJ, 224, 718
 Inoue, S., Aharonian, F. A., & Sugiyama, N. 2005, ApJ, 628, L9, arXiv:astro-ph/0505398
 Jones, C., & Forman, W. 1984, ApJ, 276, 38
 Katz, J. I. 1976, ApJ, 207, 25
 Keshet, U., Waxman, E., Loeb, A., Springel, V., & Hernquist, L. 2003, ApJ, 585, 128
 Kim, K.-T., Kronberg, P. P., & Tribble, P. C. 1991, ApJ, 379, 80
 Kushnir, D., Katz, B., & Waxman, E. 2009, Arxiv preprint arXiv:0903.2275
 Kushnir, D., & Waxman, E. 2009, Arxiv preprint arXiv:0903.2271
 Loeb, A., & Waxman, E. 2000, Nature, 405, 156
 Lutovinov, A. A., Vikhlinin, A., Churazov, E. M., Revnivtsev, M. G., & Sunyaev, R. A. 2008, ApJ, 687, 968, 0802.3742
 Navarro, J., Frenk, C., & White, S. 1997, ApJ, 490, 493
 Pfrommer, C., Ensslin, T., & Springel, V. 2008, MNRAS, 385, 1211
 Poole, G. B., Babul, A., McCarthy, I. G., Fardal, M. A., Bildfell, C. J., Quinn, T., & Mahdavi, A. 2007, MNRAS, 380, 437, arXiv:astro-ph/0701586

- Poole, G. B., Fardal, M. A., Babul, A., McCarthy, I. G., Quinn, T., & Wadsley, J. 2006, MNRAS, 373, 881, arXiv:astro-ph/0608560
- Reiprich, T., & Bohringer, H. 2002, ApJ, 567, 716
- Rephaeli, Y. 1977, ApJ, 212, 608
- . 1979, ApJ, 227, 364
- Rephaeli, Y., Nevalainen, J., Ohashi, T., & Bykov, A. M. 2008, Space Science Reviews, 134, 71, 0801.0982
- Ricker, P. M., & Sarazin, C. L. 2001, ApJ, 561, 621, arXiv:astro-ph/0107210
- Roncarelli, M., Ettori, S., Dolag, K., Moscardini, L., Borgani, S., & Murante, G. 2006, MNRAS, 373, 1339, arXiv:astro-ph/0609824
- Sarazin, C. 1999, ApJ, 520, 529
- Sarazin, C. L., & Bahcall, J. N. 1977, ApJS, 34, 451
- Sarazin, C. L., & Kempner, J. C. 2000, ApJ, 533, 73, arXiv:astro-ph/9911335
- Timokhin, A. N., Aharonian, F. A., & Neronov, A. Y. 2004, A&A, 417, 391, arXiv:astro-ph/0305149
- Vikhlinin, A., Markevitch, M., Murray, S. S., Jones, C., Forman, W., & Van Speybroeck, L. 2005, ApJ, 628, 655, arXiv:astro-ph/0412306
- Wik, D. R., Sarazin, C. L., Finoguenov, A., Matsushita, K., Nakazawa, K., & Clarke, T. E. 2009, ApJ, 696, 1700, 0902.3658